Contract No:

This document was prepared in conjunction with work accomplished under Contract No. DE-AC09-08SR22470 with the U.S. Department of Energy (DOE) Office of Environmental Management (EM).

Disclaimer:

SAVANNAH RIVER NATIONAL LABORATORY
OPERATED BY SAVANNAH RIVER NUCLEAR SOLUTIONS

September 30, 2019 SRNL-STI-2018-00681

TO: B. T. BUTCHER, 773-42A

FROM: T. L. DANIELSON, 773-42A

REVIEWER: J. A. DYER, 773-42A

L. L. HAMM, 735-A

Recommendation 150, 155, 157

RECOMMENDED STRATEGY FOR IMPLEMENTING PORFLOW SUBSIDENCE INFILTRATION BOUNDARY CONDITIONS

Scope

This technical memorandum summarizes a limited-in-scope sensitivity analysis that addresses uncertainty in the conservatism of blending infiltration rates for use as input boundary conditions in PORFLOW vadose zone simulations as opposed to blending flux-to-the-water-table outputs for different subsidence infiltration scenarios, as has been done historically.

Results / Conclusions

PORFLOW vadose zone contaminant transport simulations produced time-dependent flux-to-the-water-table profiles for nine infiltration implementations. Subsequent blending of the flux-to-the-water-table profiles for nine radionuclides allowed comparison of the methodology used in the 2018 Special Analysis (SA) of the E-Area Low-Level Waste Facility (LLWF) (Hamm et al., 2018) and the methodology used historically (e.g., in the 2008 E-Area Performance Assessment). The comparison shows that the methodology used by Hamm et al. (2018) is a more conservative (i.e., results in higher radionuclide flux to the water table) implementation of subsidence.

Discussion

Background

PORFLOW (ACRi, 2010) simulations in the 2018 SA of the E-Area LLWF (Hamm et al., 2018) were constructed using a bounding conceptual infiltration model identified by Dyer (2017). Based on guidance

from this model, a longitudinal cross-section from a geometric section of the proposed E-Area LLWF final closure cap was selected to represent both slit and engineered trenches. The proposed final closure cap is shown in Figure 1 where the bounding geometry is outlined in blue and arrows indicate the orientation of the longitudinal cross-section. This portion of the cap has an off-centered crest with two significantly different slope lengths – a 585-foot-long slope and a 150-foot-long slope (40-foot overhangs at both ends are always considered intact, i.e., no subsidence occurs). Under subsidence conditions, the combined surface and lateral-drainage-layer runoff (into the subsided area or hole) from upslope portions of the intact cap varies significantly for these two slope lengths; therefore, each slope requires a unique infiltration rate to adequately describe infiltration across the overall cap.

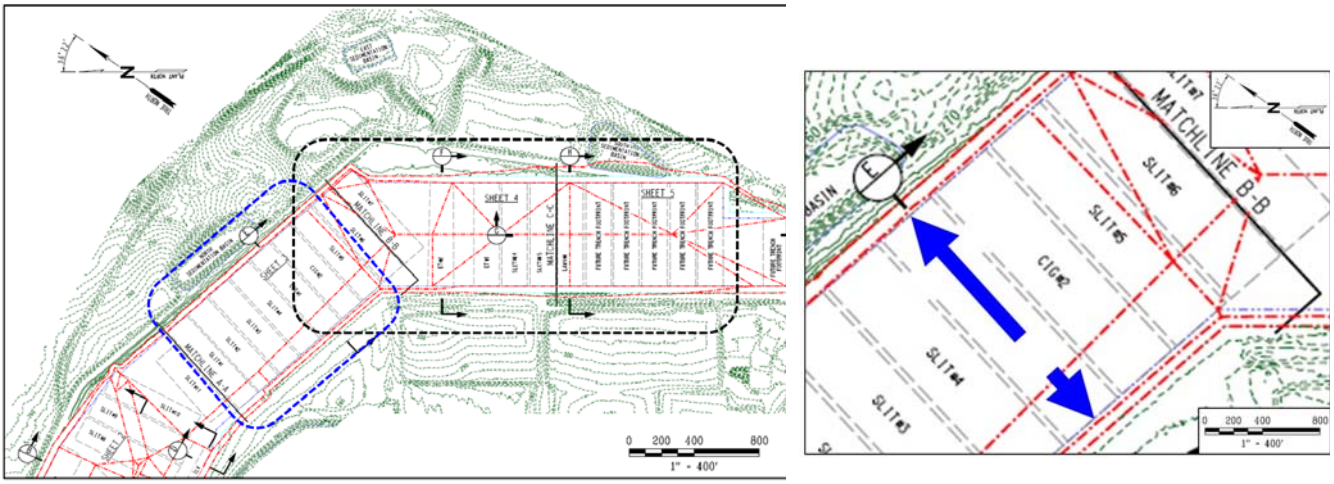

Figure 1. The proposed final closure cap design (indicated by red lines) for the E-Area LLWF. The section of the cap corresponding to the geometry that bounds the infiltration model is outlined in blue. Disposal units of interest in the 2018 SA are outlined in black. Long and short blue arrows show the direction of runoff flow for the long and short slopes of the longitudinal slice.

Two unique implementations of subsidence boundary conditions were considered in PORFLOW vadose zone flow simulations:

1) Case11a – a slope-length-weighted, cap-averaged infiltration rate applied across the entire length of the disposal unit.
2) Case11b – a back-calculated infiltration rate (based on the Case11a infiltration rate) applied to a discrete 12-foot hole located in the center of the disposal unit.

The slope-length-weighted, cap-averaged infiltration rate of Case11a was supplied from the outputs of the combined deterministic/probabilistic approach developed by Dyer and Flach (2018). Within their approach, intact infiltration rates were calculated directly using the Hydrologic Evaluation of Landfill Performance (HELP) model (Dixon, 2017). Monte Carlo simulations were conducted using 100,000

realizations, thereby capturing a statistical distribution of possible hole locations and upslope-intact-area slope lengths. From this, the average infiltration rate across all 100,000 realizations was obtained for each slope length. Subsequently, the average infiltration rates for the 110-foot slope and the 545-foot slope were averaged together (weighted by their fractional contribution to the entire cap length) to give the slope-length-weighted, cap-averaged infiltration rates (i.e., inputs for Case11a) for 2.0%, 0.6%, and 0.04% subsidence scenarios. The cap-averaged infiltration rates were then used to back-calculate the infiltration rate for a discrete 12-foot hole (~1.8% of the total cap length, regardless of percent subsidence infiltration rate) centrally located along the disposal unit length as:

$$I_D = \frac{I_{Av} - 0.982 I_I}{0.018}$$

where, I_{Av} and I_I are the slope-length-weighted, cap-averaged infiltration rate and the intact infiltration rate, respectively.

Following the usual method of running PORFLOW vadose zone and aquifer simulations, the infiltration rates for Case11a and Case11b were applied in a sequence of steady-state flow simulations that were subsequently used as input to transient vadose zone contaminant transport simulations. From this, time-dependent fluxes to the water table for the radionuclides of interest were obtained and later used directly as source input terms in aquifer transport simulations.

Earlier treatments of subsidence, such as in the 2008 Performance Assessment (WSRC, 2008) of the E-Area LLWF, employed alternative methods for modeling subsidence. Intact and subsided infiltration rate boundary conditions were obtained from the HELP model and applied across the PORFLOW model domain in separate simulations (i.e., two separate sequences of steady-state flow simulations with different boundary conditions were fed to transient transport simulations). Subsequently, the time-dependent fluxes to the water table for the subsided and intact cases were blended with a 9:1 intact-to-subsided ratio to obtain 10% subsidence source inputs for aquifer transport simulations.

Comparing the two methods, the primary difference is whether blending is performed on the input (new method) or on the output (historical method) of the PORFLOW simulations. To ensure that the new conceptual infiltration model accounts for subsidence in an appropriately conservative manner, a number of test cases were explored that blend the infiltration rates in different ways, some of which mirror the historical method by blending outputs as opposed to blending the inputs. For the purposes of this limited-in-scope sensitivity study, only the 2% subsidence scenario was tested using the disposal unit timeline for Slit Trench No. 14 (Hamm et al. (2018) further describes the disposal-unit-specific inputs).

Boundary Condition Formulations

The calculated infiltration rates from the combined deterministic/probabilistic approach of Dyer and Flach (2018) are shown in Table 1. Time-dependent intact infiltration rates were supplied directly as output from HELP model simulations and the long- and short-slope-averaged infiltration rates were supplied directly as output from Monte Carlo simulations. Cap-averaged infiltration rates used in Case11a by Hamm et al. (2018) were obtained from a slope-length-weighted average of the long- and short-slope average infiltration rates. On the other hand, the back-calculated subsided-area (hole) infiltration rates used in Case11b by Hamm et al. (2018) were calculated using the cap-averaged infiltration rate.

Table 1. Infiltration rates calculated from the combined deterministic/probabilistic approach by Dyer and Flach (2018).

Relative Year	Intact Infiltration Rate (inches/year)	Long-Slope-Averaged Infiltration Rate (inches/year)	Short-Slope-Averaged Infiltration Rate (inches/year)	Cap-Averaged Infiltration Rate (inches/year) *(Case11a)*	Back-Calculated Infiltration Rate for Hole (inches/year) *(Case11b)*
0	15.780	15.780	15.780	15.780	15.780
30	0.100	0.100	0.100	0.100	0.100
171	0.001	6.666	1.856	5.858	325.392
251	0.008	6.623	1.865	5.824	323.139
361	0.189	6.732	1.999	5.938	319.561
371	0.204	6.762	2.058	5.972	320.622
411	0.322	6.800	2.154	6.020	316.882
451	0.405	6.873	2.221	6.092	316.315
551	1.457	7.498	3.171	6.771	296.669
731	3.230	8.577	4.711	7.928	264.221
1171	7.015	10.845	8.074	10.380	193.956

The top boundary of the PORFLOW mesh was subdivided into twelve infiltration zones for specifying the boundary conditions; however, only the six zones along the length of the disposal unit differ from those used by Hamm et al. (2018). Figure 2 highlights the approximate location of the infiltration zones along the length of the disposal unit. Regions 1, 2, and 3 represent the final closure cap from the left edge of the disposal unit to the cap crest (i.e., the short slope), with Region 2 representing a 12.25-foot-long subsided hole location. Regions 4, 5, and 6 represent the final closure cap from the cap crest to the right

edge of the disposal unit (i.e., the long slope), with Region 5 representing a 12.27-foot-long subsided hole location. (Hamm et al. (2018) provides more information on the PORFLOW model geometry, material properties specifications, timeline, etc.)

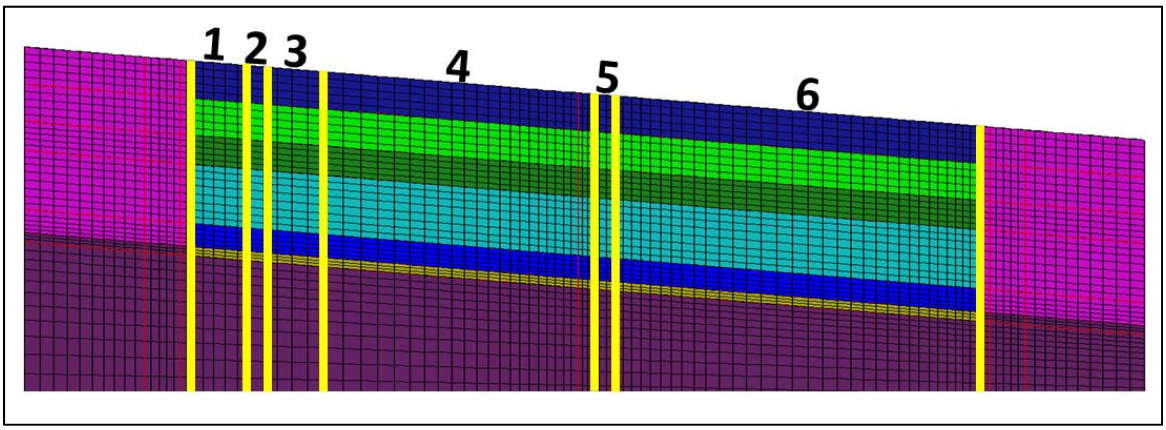

Figure 2. Six infiltration boundary regions along the length of the disposal unit where subsidence infiltration conditions are applied.

Using the infiltration rates from Table 1 and a combination of eight different boundary condition formulations (Table 2, Table 3, and Table 4), nine separate cases (Figure 3) were created and run through PORFLOW vadose zone flow and transport. As a result, time-dependent fluxes to the water table were obtained for the same nine radionuclides explored by Hamm et al. (2018).

Table 2. The boundary condition formulation that is applied in PORFLOW to each of the six infiltration regions over the disposal unit for each unique infiltration case.

		Regions					
		1	2	3	4	5	6
Cases	1	I_{Av-SS}	I_{Av-SS}	I_{Av-SS}	I_{Intact}	I_{BC-LS}	I_{Intact}
	2	I_{Intact}	I_{BC-SS}	I_{Intact}	I_{Av-LS}	I_{Av-LS}	I_{Av-LS}
	3	I_{Av-SS}	I_{Av-SS}	I_{Av-SS}	I_{Av-LS}	I_{Av-LS}	I_{Av-LS}
	4	I_{Av-LS}	I_{Av-LS}	I_{Av-LS}	I_{Av-LS}	I_{Av-LS}	I_{Av-LS}
	5	I_{Av-SS}	I_{Av-SS}	I_{Av-SS}	I_{Av-SS}	I_{Av-SS}	I_{Av-SS}
	6	I_{Intact}	I_{Intact}	I_{Intact}	I^{MB}_{Av-LS}	I^{MB}_{Av-LS}	I^{MB}_{Av-LS}
	7	I^{MB}_{Av-SS}	I^{MB}_{Av-SS}	I^{MB}_{Av-SS}	I_{Intact}	I_{Intact}	I_{Intact}
	8	I_{Intact}	I_{Intact}	I_{Intact}	I_{Intact}	I^{MB}_{BC-LS}	I_{Intact}
	9	I_{Intact}	I^{MB}_{BC-SS}	I_{Intact}	I_{Intact}	I_{Intact}	I_{Intact}

Table 3. Description of the eight different boundary condition formulations.

Boundary Condition Description	Formulation
Monte Carlo Long-Slope-Averaged Infiltration Rate	I_{Av-LS} (Table 1)
Monte Carlo Short-Slope-Averaged Infiltration Rate	I_{Av-SS} (Table 1)
Long Slope Back-Calculated Infiltration Rate	$I_{BC-LS} = \frac{I_{Av-LS} - \left(\frac{L_{LongSlope} - L_{Subsided}}{L_{LongSlope}}\right) I_{Intact}}{\frac{L_{Subsided}}{L_{LongSlope}}}$
Short Slope Back-Calculated Infiltration Rate	$I_{BC-SS} = \frac{I_{Av-SS} - \left(\frac{L_{ShortSlope} - L_{Subsided}}{L_{ShortSlope}}\right) I_{Intact}}{\frac{L_{Subsided}}{L_{ShortSlope}}}$
*Mass Balanced Long-Slope-Averaged Infiltration Rate**	$I^{MB}_{Av-LS} = \frac{I_{AvCap} L_{Total} - I_{Intact} L_{ShortSlope}}{L_{LongSlope}}$
*Mass Balanced Short-Slope-Averaged Infiltration Rate**	$I^{MB}_{Av-SS} = \frac{I_{Av-Cap} L_{Total} - I_{Intact} L_{LongSlope}}{L_{ShortSlope}}$
*Mass Balanced Long Slope Back-Calculated Infiltration Rate**	$I^{MB}_{BC-LS} = \frac{I_{Intact} L_{ShortSlope} + I^{MB}_{Av-LS} L_{LongSlope} - L_{Intact} I_{Intact}}{L_{Subsided}}$
*Mass Balanced Short Slope Back-Calculated Infiltration Rate**	$I^{MB}_{BC-SS} = \frac{I_{Intact} L_{LongSlope} + I^{MB}_{Av-SS} L_{ShortSlope} - L_{Intact} I_{Intact}}{L_{Subsided}}$

I_{Av-LS} =Averaged infiltration rate of the long slope from Table 1

I_{Av-SS} =Averaged infiltration rate of the short slope from Table 1

I_{Intact} = Intact infiltration rate from Table 1

I_{Av-Cap} =*Slope-length-weighted, cap-averaged infiltration rate from Table 1*

$L_{LongSlope}$ =*Length of the long slope (i.e., 545 feet)*

$L_{ShortSlope}$ =*Length of the short slope (i.e., 110 feet)*

L_{Total} =*Total length of the cap covering the disposal unit (i.e., 655 feet)*

$L_{Subsided}$ =*Length of the subsided area (hole)*

L_{Intact} =*Length of the cap over the DU that is intact*

[*] *See Appendix A for derivation*

Table 4. The calculated infiltration rates based on the infiltration formulations shown in Table 3.

Relative Year	I_{BC-LS} (in/yr)	I_{BC-SS} (in/yr)	I^{MB}_{Av-LS} (in/yr)	I^{MB}_{Av-SS} (in/yr)	I^{MB}_{BC-LS} (in/yr)	I^{MB}_{BC-SS} (in/yr)
0	15.780	15.780	15.780	15.780	15.780	15.780
30	0.100	0.100	0.100	0.100	0.100	0.100
171	296.032	16.659	7.038	34.930	313.215	313.718
251	293.848	16.685	6.996	34.695	311.047	311.547
361	290.836	16.447	7.096	34.472	307.609	308.103
371	291.469	16.850	7.134	34.600	308.632	309.127
411	288.072	16.774	7.168	34.303	305.035	305.525
451	287.674	16.714	7.237	34.317	304.493	304.982
551	269.760	16.842	7.842	33.147	285.621	286.078
731	240.736	16.525	8.874	31.246	254.454	254.858
1171	177.146	16.522	11.058	27.082	186.960	187.249

Blending Scenario 1

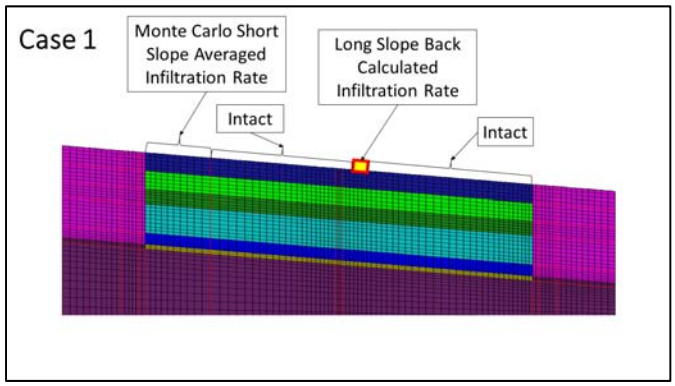

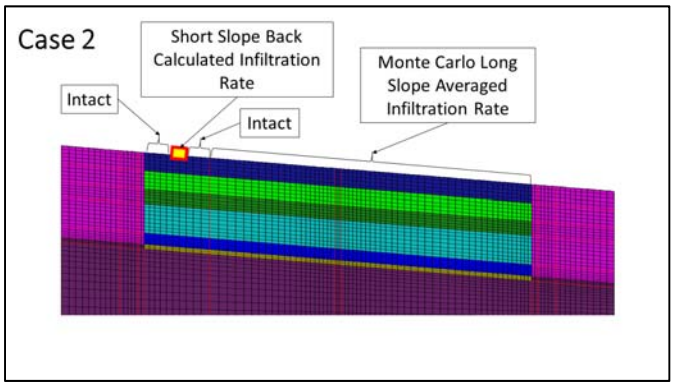

Blending Scenario 2

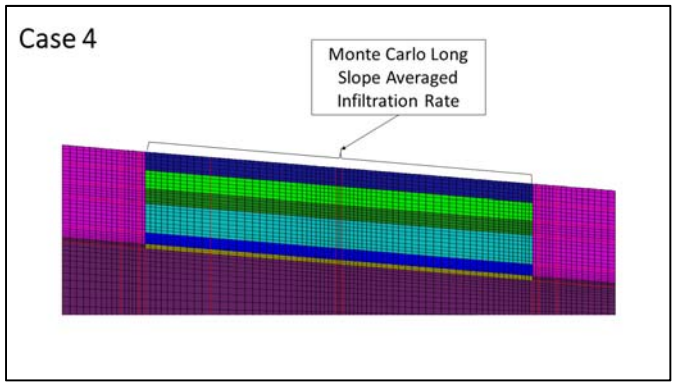

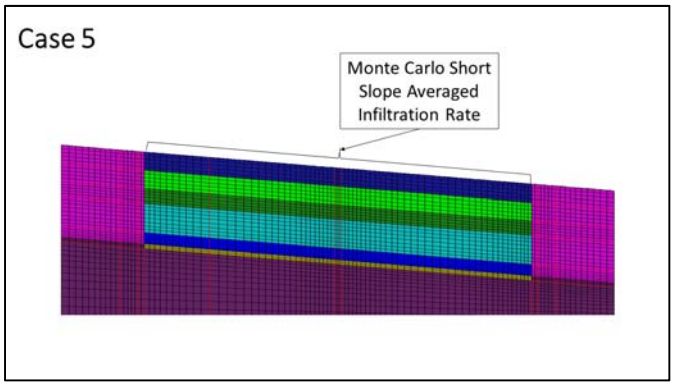

Blending Scenario 3

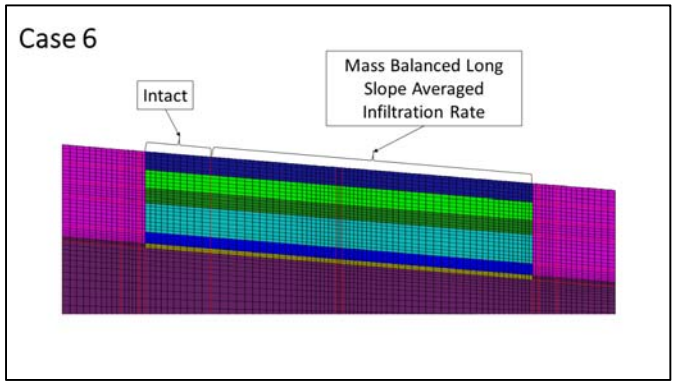

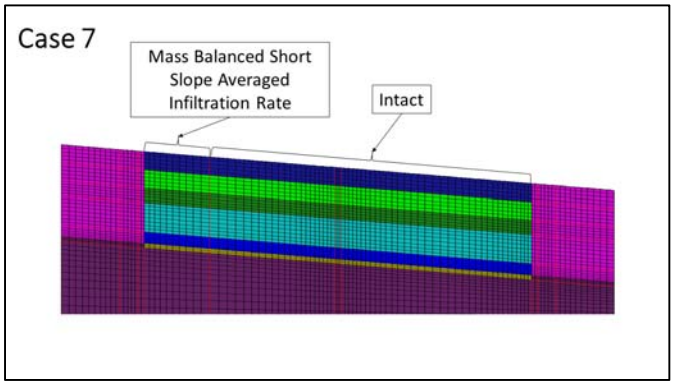

Blending Scenario 4

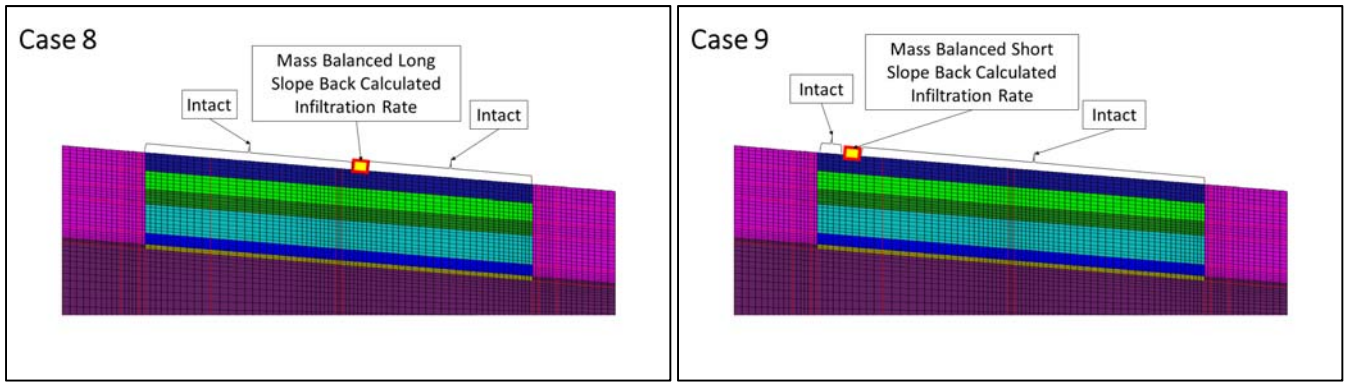

Non-Blending Scenario

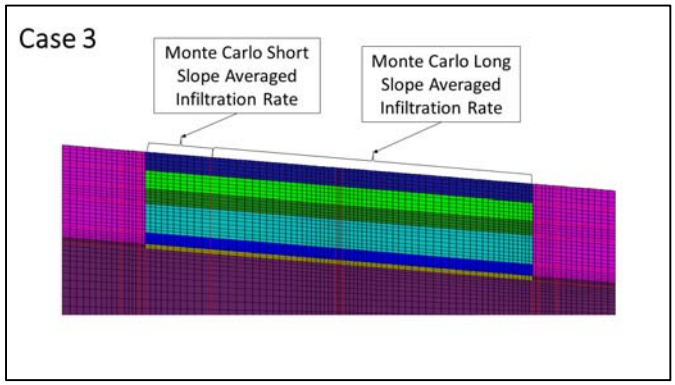

Figure 3. Illustration of nine infiltration cases and four blending scenarios. For cases grouped as pairs, blending of the flux-to-the-water-table outputs was performed. No blending was performed for Case 3.

With the exception of Case 3 (which has no blending), the cases shown in Figure 3 are grouped according to corresponding pairs of simulations for which blending of the fluxes to the water table was performed. For all blended scenarios, the case on the left is blended with the case on the right (using Case 1 and Case 2 as an example):

$$Flux_{Blended} = \frac{Flux_1(t) \times 545 + Flux_2(t) \times 110}{655}$$

To directly compare the blended radionuclide fluxes to the water table to Case11a and Case11b from Hamm et al. (2018), the water balance (i.e., the total mass or volume of water input to the system) must be the same across all blending scenarios. To confirm the water balance in scenarios where blending was performed, the length of a given infiltration boundary region (Figure 2) was multiplied by the infiltration

rate applied to that region and summed across all regions to give the total volume (mass) of water (expressed in cubic inches per year (in^3/yr) assuming the longitudinal slice is one-inch thick). Subsequently, the total volume of water for the case on the left was blended with the case on the right (in the same way as the flux to the water table) to obtain the total amount of water in the blended scenario. Comparison to the total volume of water in Case11a and Case11b shows the mass balance is equal to within a fraction of one percent.

The deterministic/probabilistic approach of Dyer and Flach (2018) assumes equal likelihood that subsidence occurs at all locations across the cap. As such, the averaged infiltration rates for the short and long slopes are averaged infiltration rates assuming 2% subsidence (for this study) on the short slope and 2% subsidence on the long slope, respectively. Combining the two, the slope-length-weighted, cap-averaged infiltration rate is representative of 2% subsidence across the entire surface of the cap covering the disposal unit. Therefore, it is possible to blend, using a satisfactory water balance, any two cases where each slope length has an appropriate specification of 2% subsidence, as is implemented in Case 1 + Case 2, Case 3, and Case 4 + Case 5. On the other hand, if the average infiltration rate for the short slope is applied to the short slope and the remainder of the cap is specified as intact, the total amount of water infiltrating through the cap is under-represented (i.e., overall cap-average less than 2% subsidence). Therefore, the infiltration rate must be calibrated to the slope-length-weighted, cap-averaged value so that an infiltration rate representative of 2% subsidence is applied to the slope of interest, as has been done in Case 6 + Case 7 and Case 8 + Case 9 (see Appendix A for the derivation of the averaged and back-calculated infiltration rates used in these cases).

Vadose Zone Transport Results

The blended flux to the water table for Case(s) 1 – 9 are shown in Figure 5 through Figure 16. Notably, for all radionuclides, except H-3, either Case11a or Case11b is the most conservative subsidence infiltration implementation. For H-3, Case 3 is the most conservative subsidence implementation; however, the difference is only approximately 3 percent when compared to Case11a. This difference is considered negligible because the *absolute* peak occurs before the installation of the final cover. Case 3 has no blending and H-3 moves unretarded through the vadose zone. When the final cover is installed, the long-slope infiltration rate for Case 3 is 6.666 in/yr, compared to the slope-length-weighted, cap-averaged infiltration rate of 5.858 in/yr. Because greater than 80% of the waste is covered by the long slope, the higher infiltration rate assumed in Case 3 transports H-3 from the waste forms at an earlier time, resulting in a slightly higher peak.

Figure 4 illustrates why blending the fluxes to the water table results in a less conservative implementation of subsidence than blending the infiltration rates. Consider Series 1 and Series 2 to be analogous to individual flux-to-the-water-table curves for two cases that are to be blended. Series 3 represents the blending of Series 1 and Series 2 via the same blending scheme utilized on PORFLOW flux-to-the-water-

table results, where Series 2 is given the blending weight of 110/655 and Series 1 is given the blending weight of 545/655. By blending using fractional weights (i.e., numbers less than 1.0), the absolute maximum of the combined curve is *required* to be less than that of either Series 1 or Series 2.

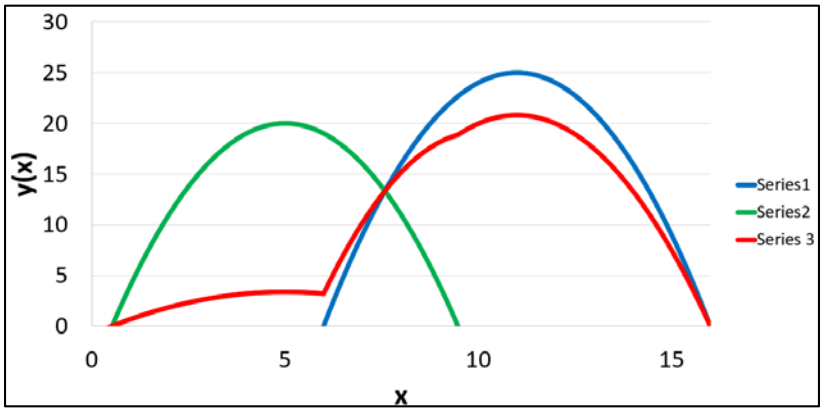

Figure 4. Illustration of blending flux to the water table with fractional weights.

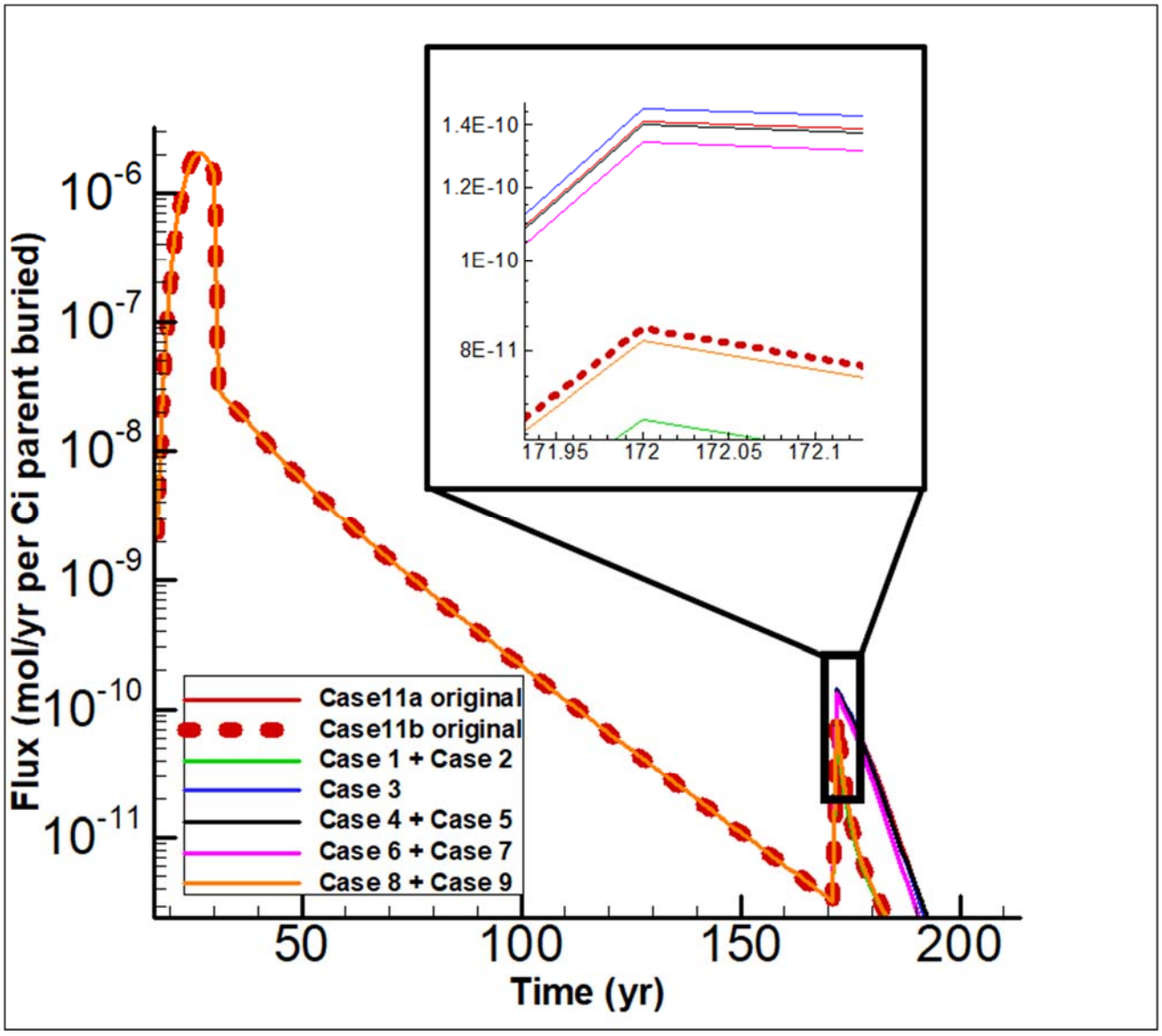

Figure 5. Comparison H-3 flux-to-the-water-table results.

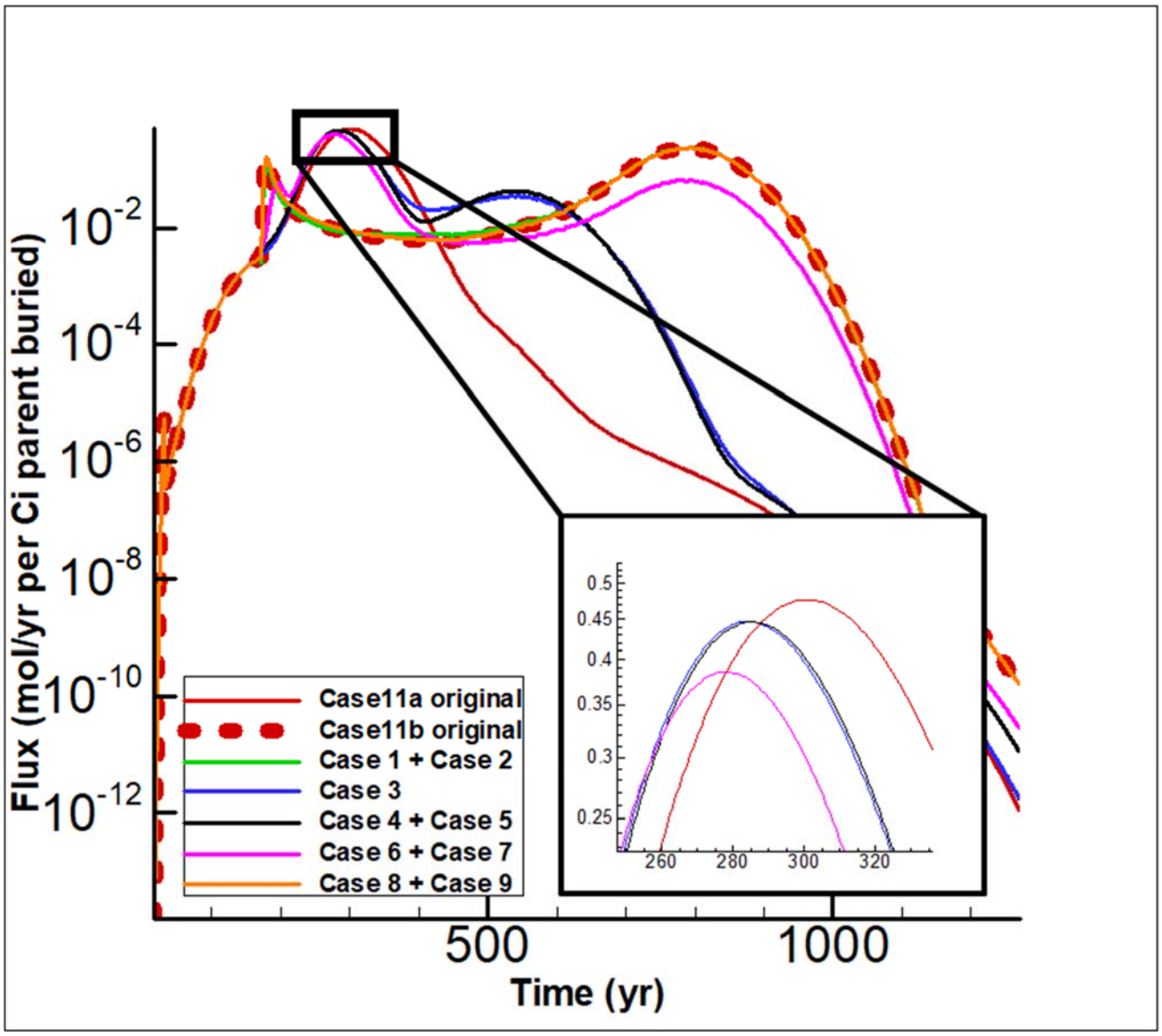

Figure 6. Comparison I-129 flux-to-the-water-table results.

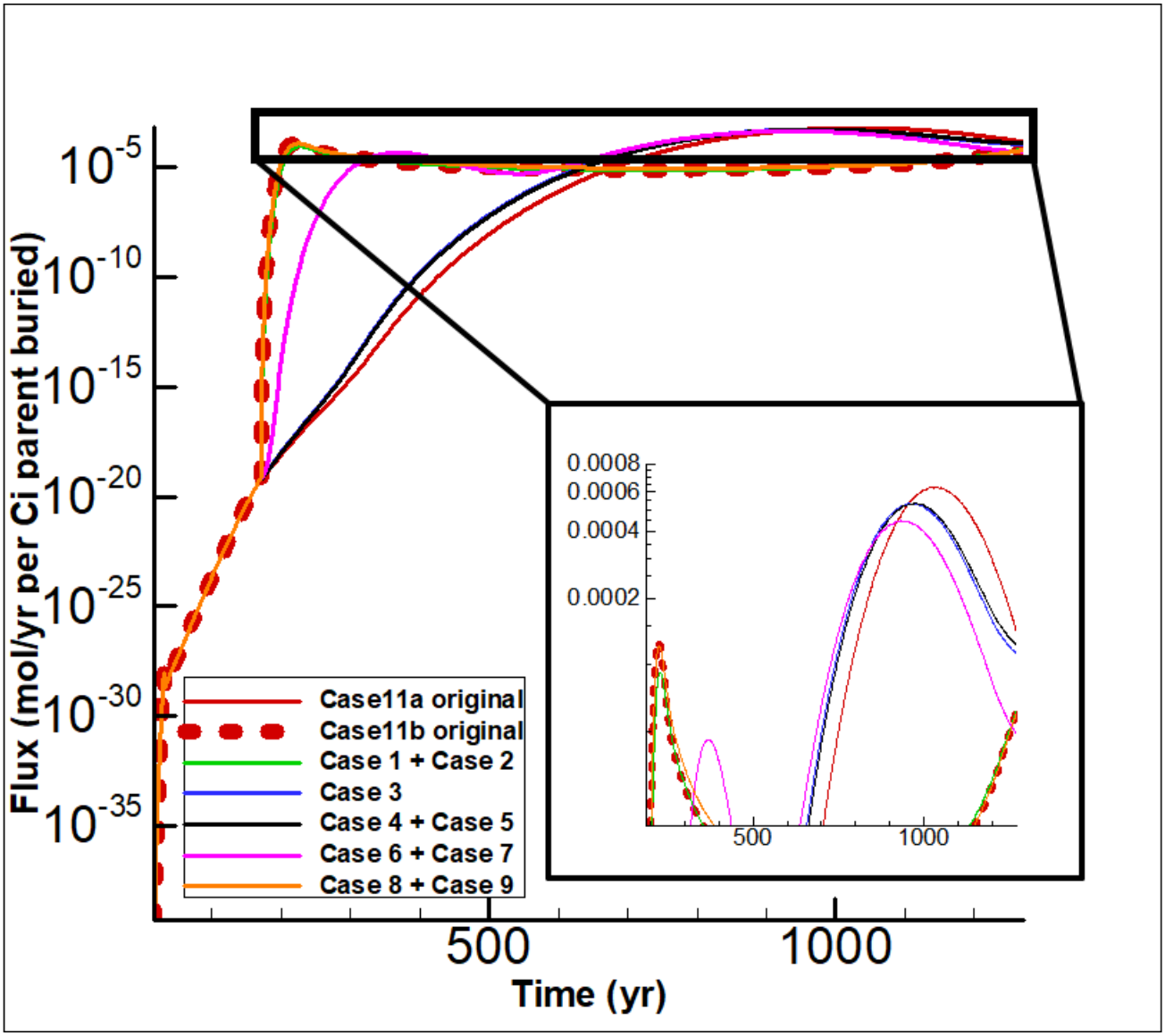

Figure 7. Comparison Ni-59 flux-to-the-water-table results.

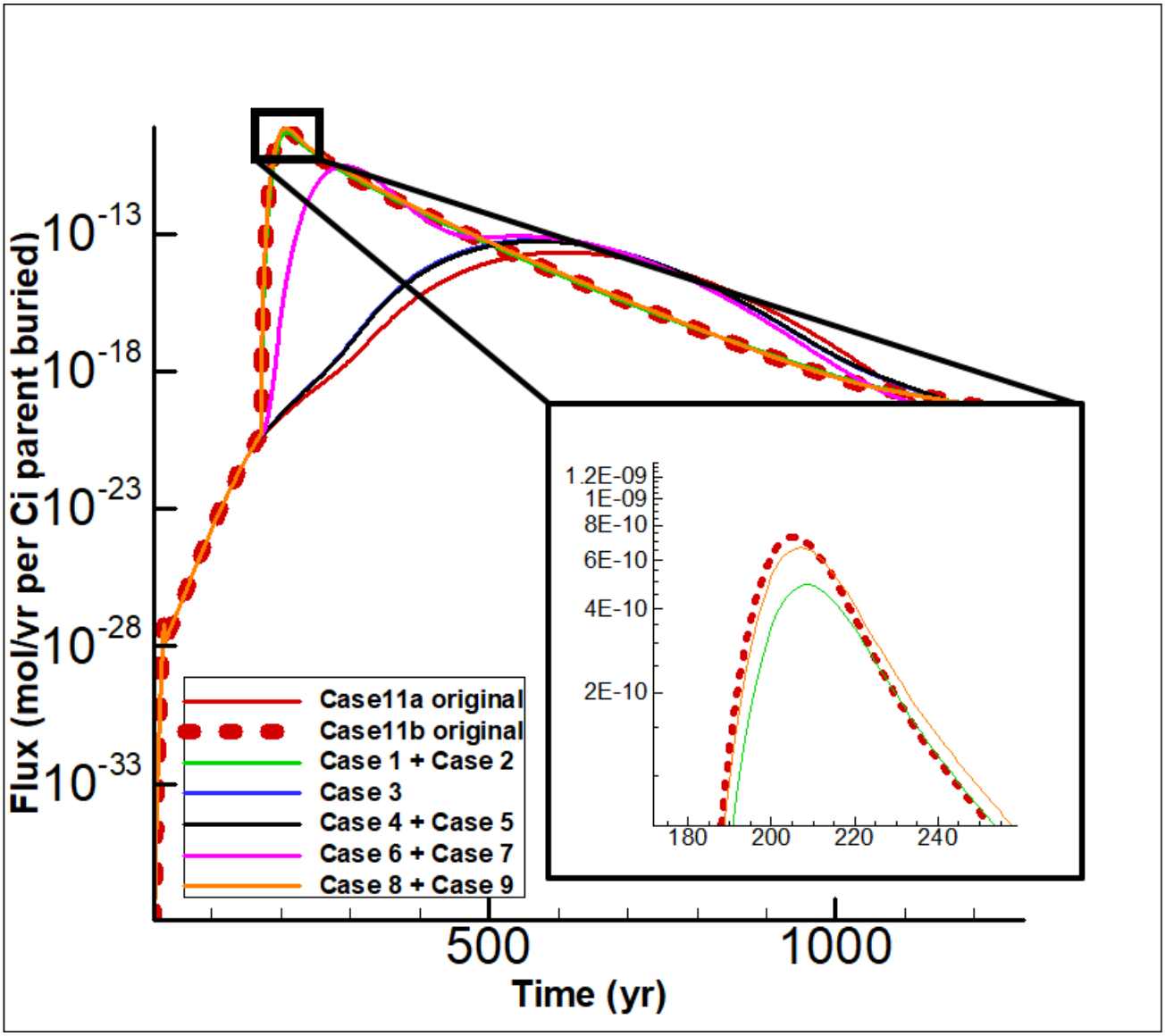

Figure 8. Comparison Sr-90 flux-to-the-water-table results.

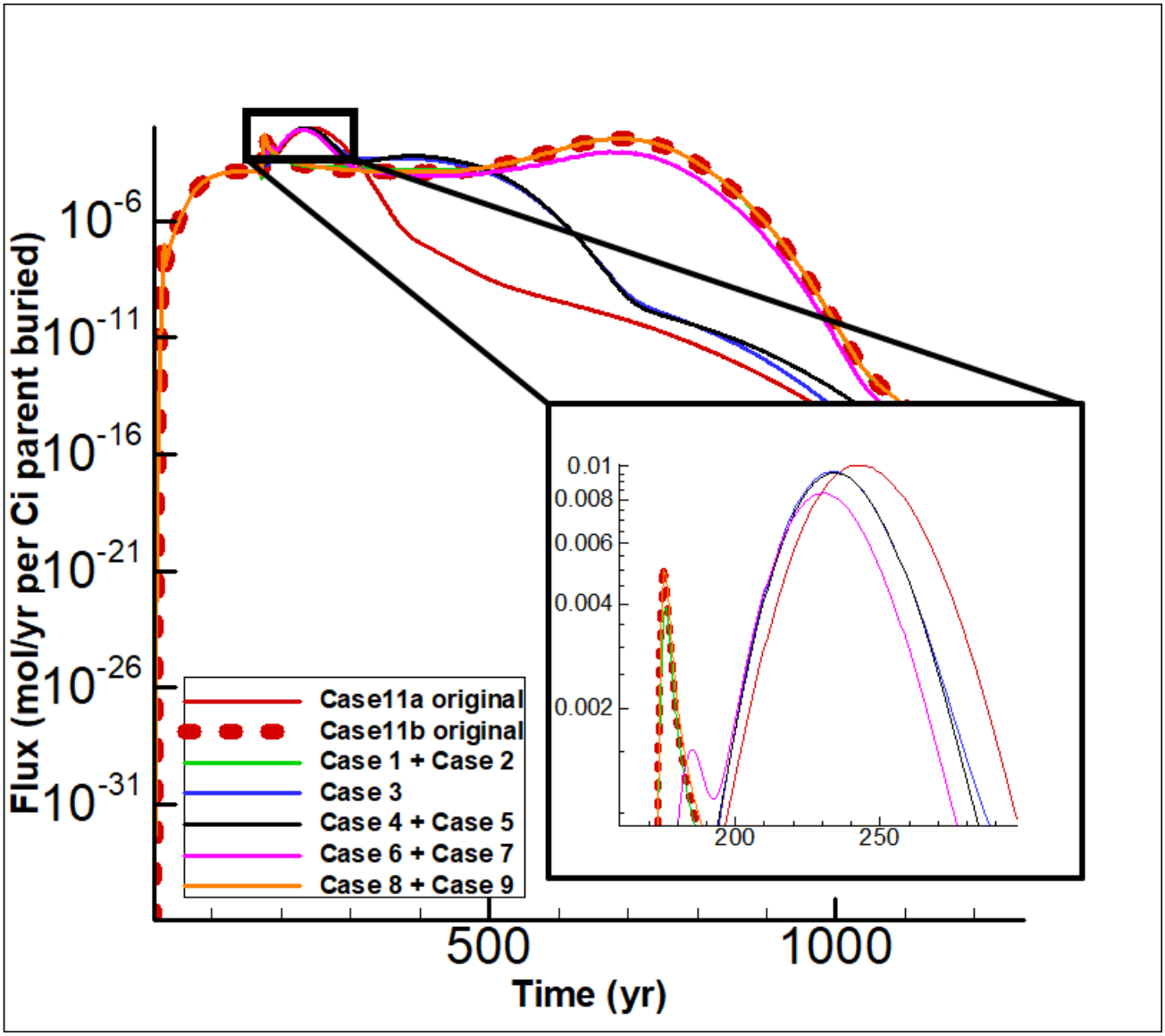

Figure 9. Comparison Tc-99 flux-to-the-water-table results.

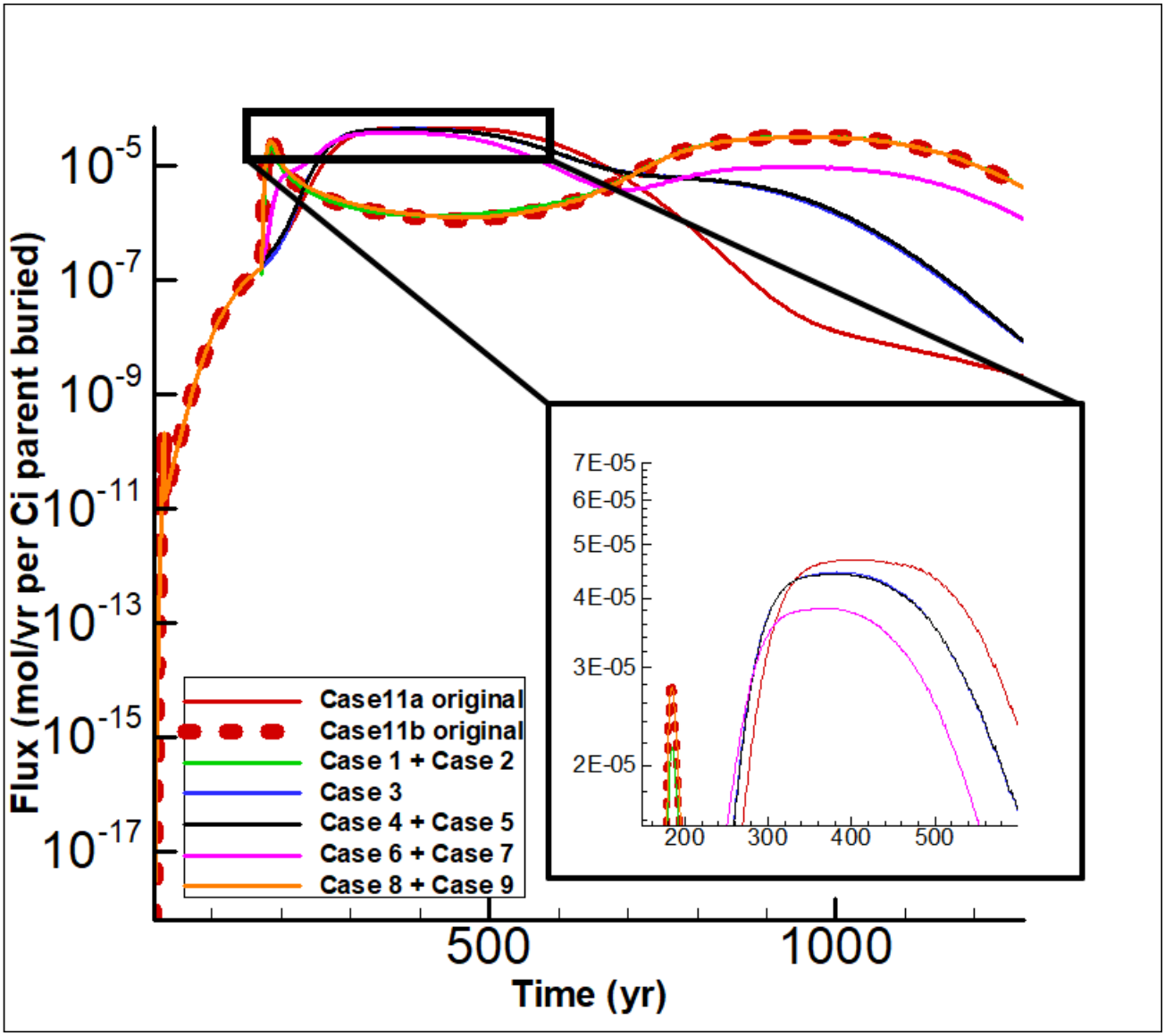

Figure 10. Comparison C-14 flux-to-the-water-table results.

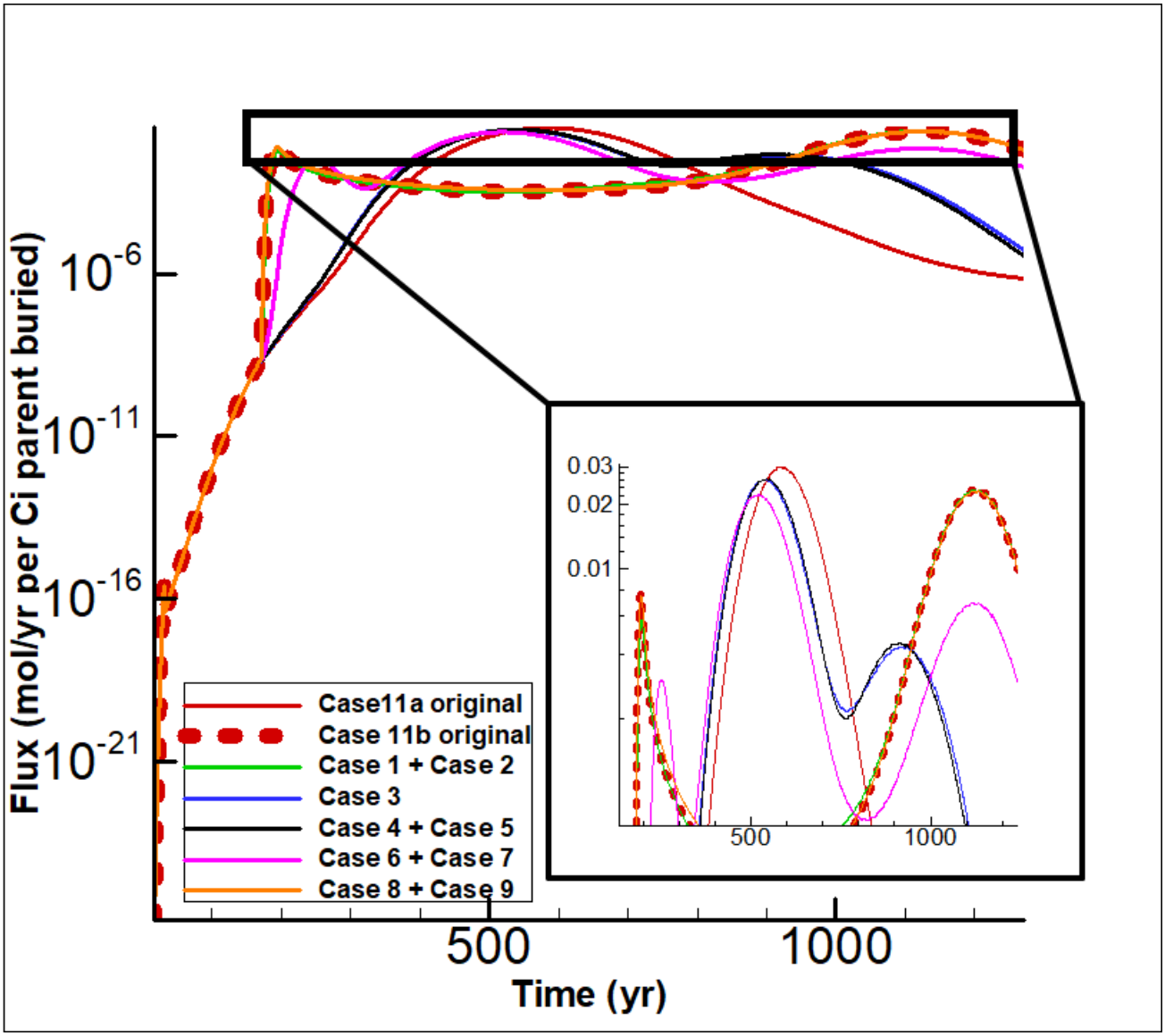

Figure 11. Comparison Np-237 (parents) flux-to-the-water-table results.

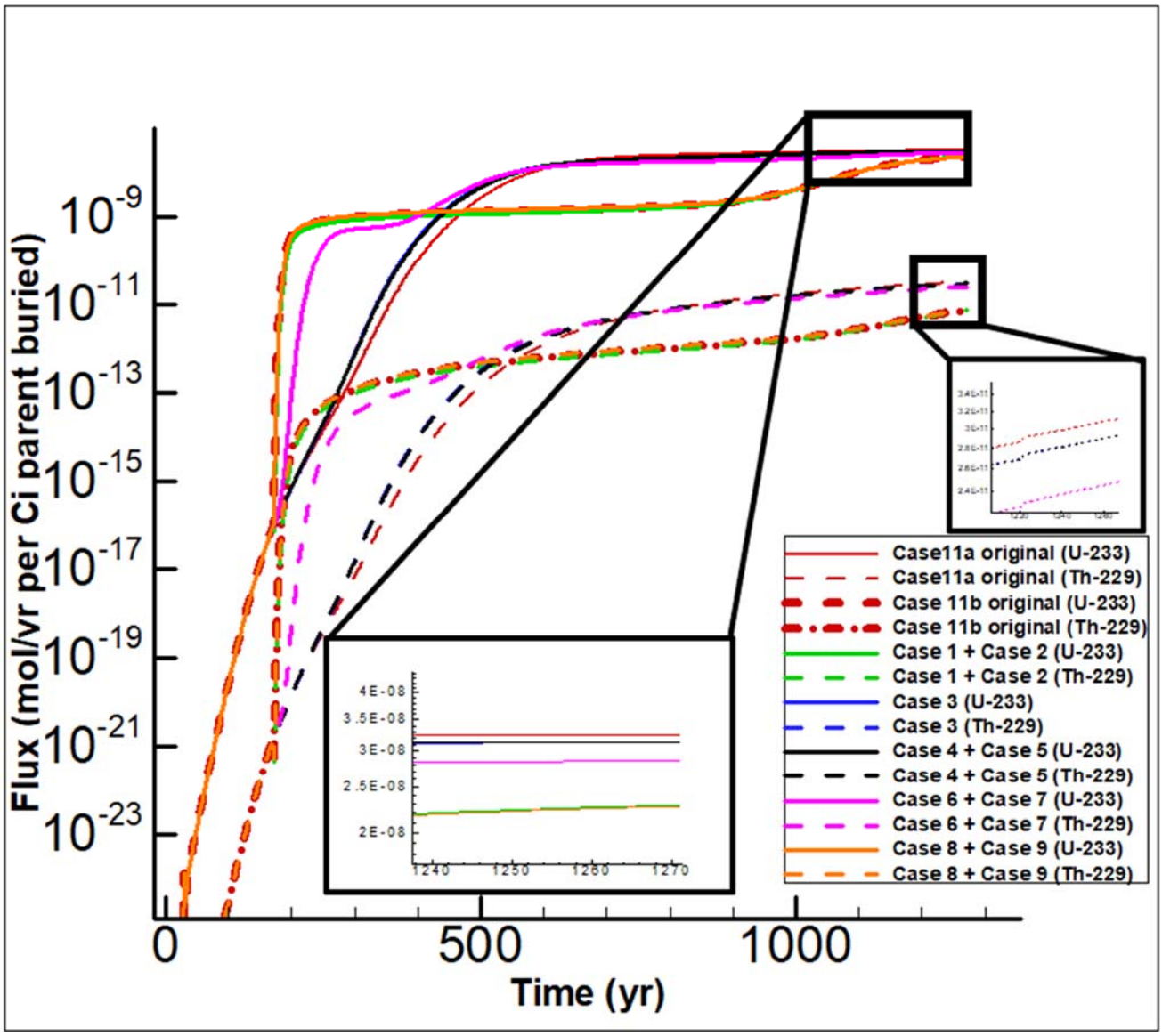

Figure 12. Comparison Np-237 (progeny) flux-to-the-water-table results.

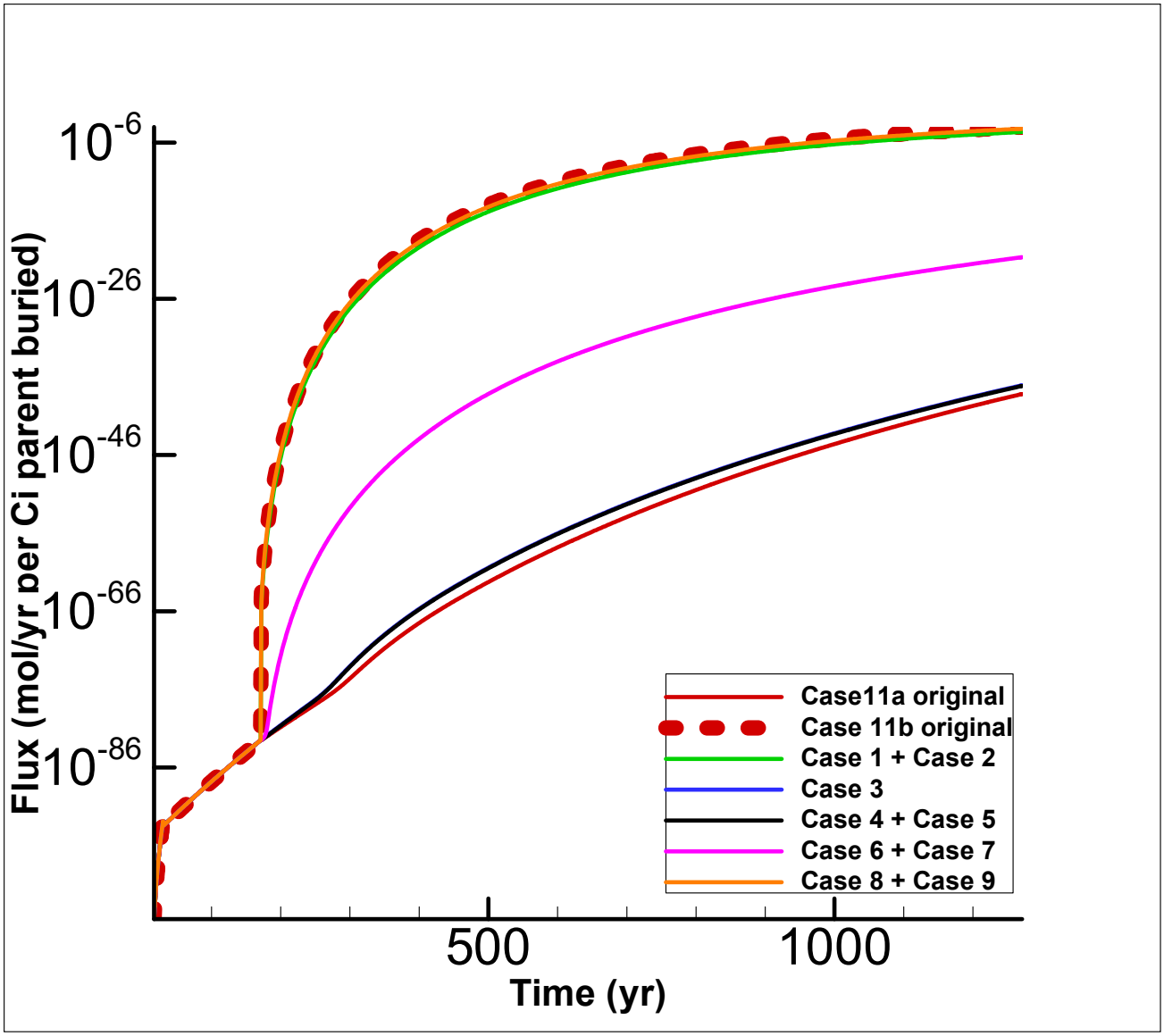

Figure 13. Comparison U-235 (parents) flux-to-the-water-table results.

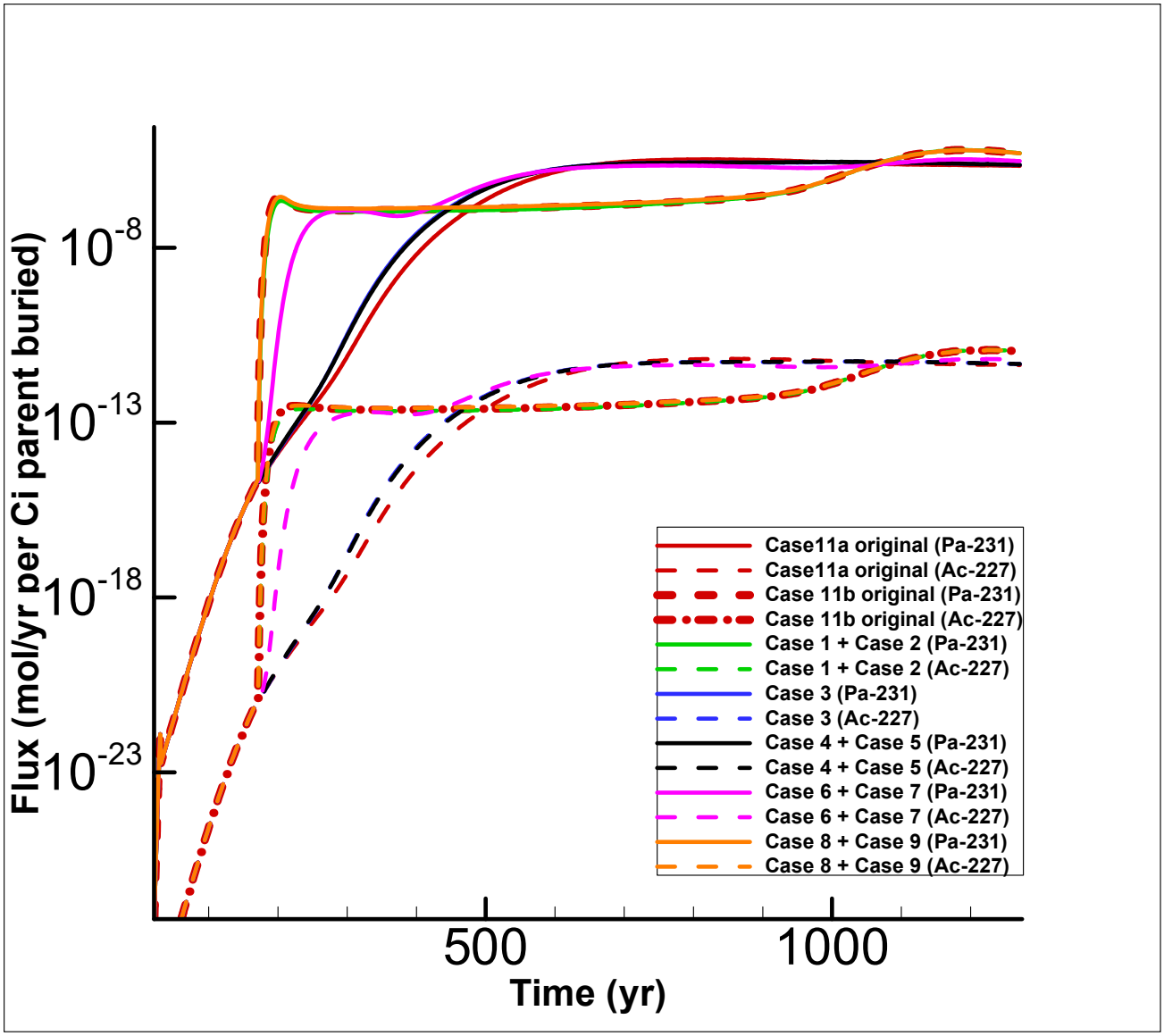

Figure 14. Comparison U-235 (progeny) flux-to-the-water-table results.

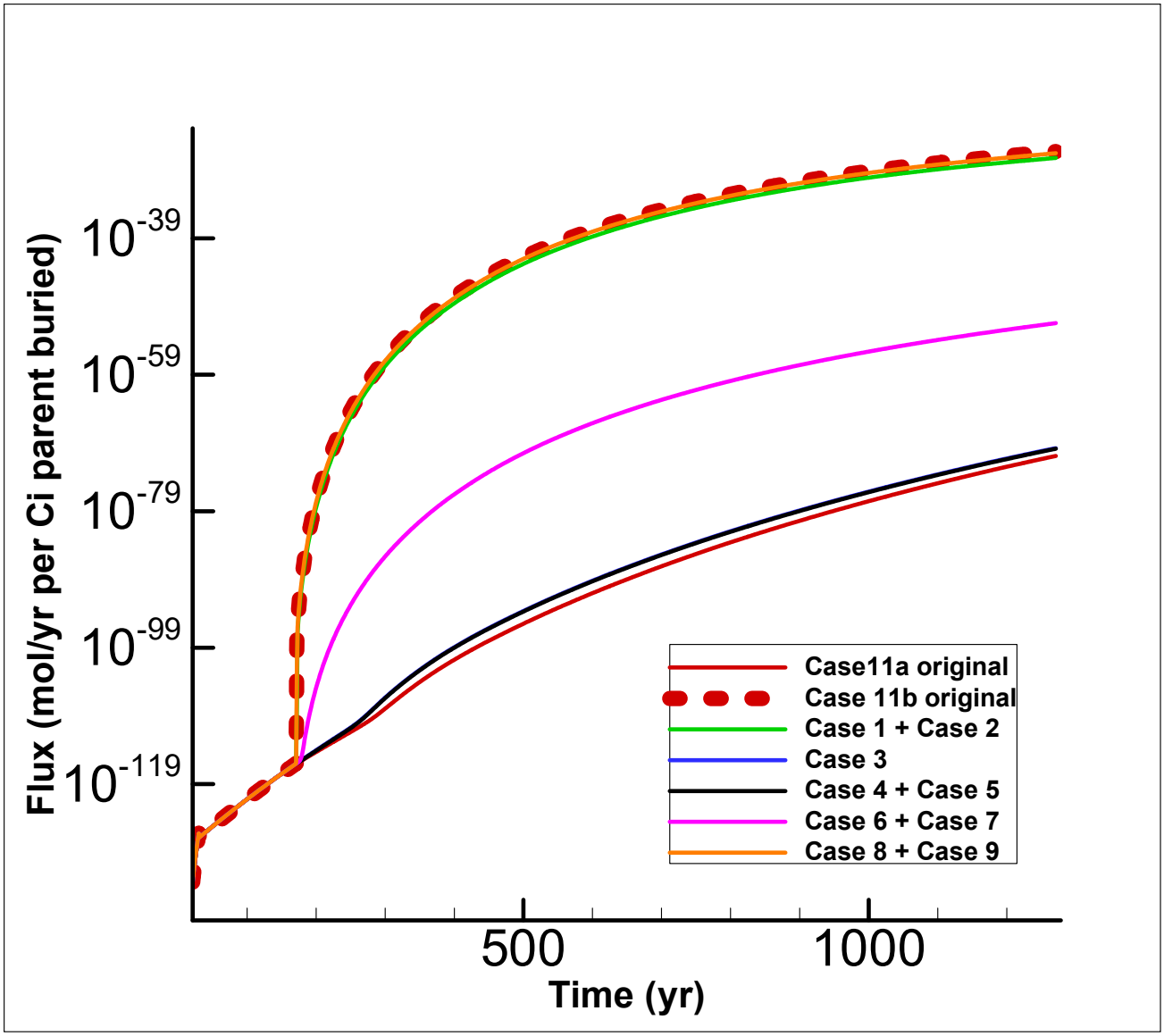

Figure 15. Comparison Am-241 (parents) flux-to-the-water-table results.

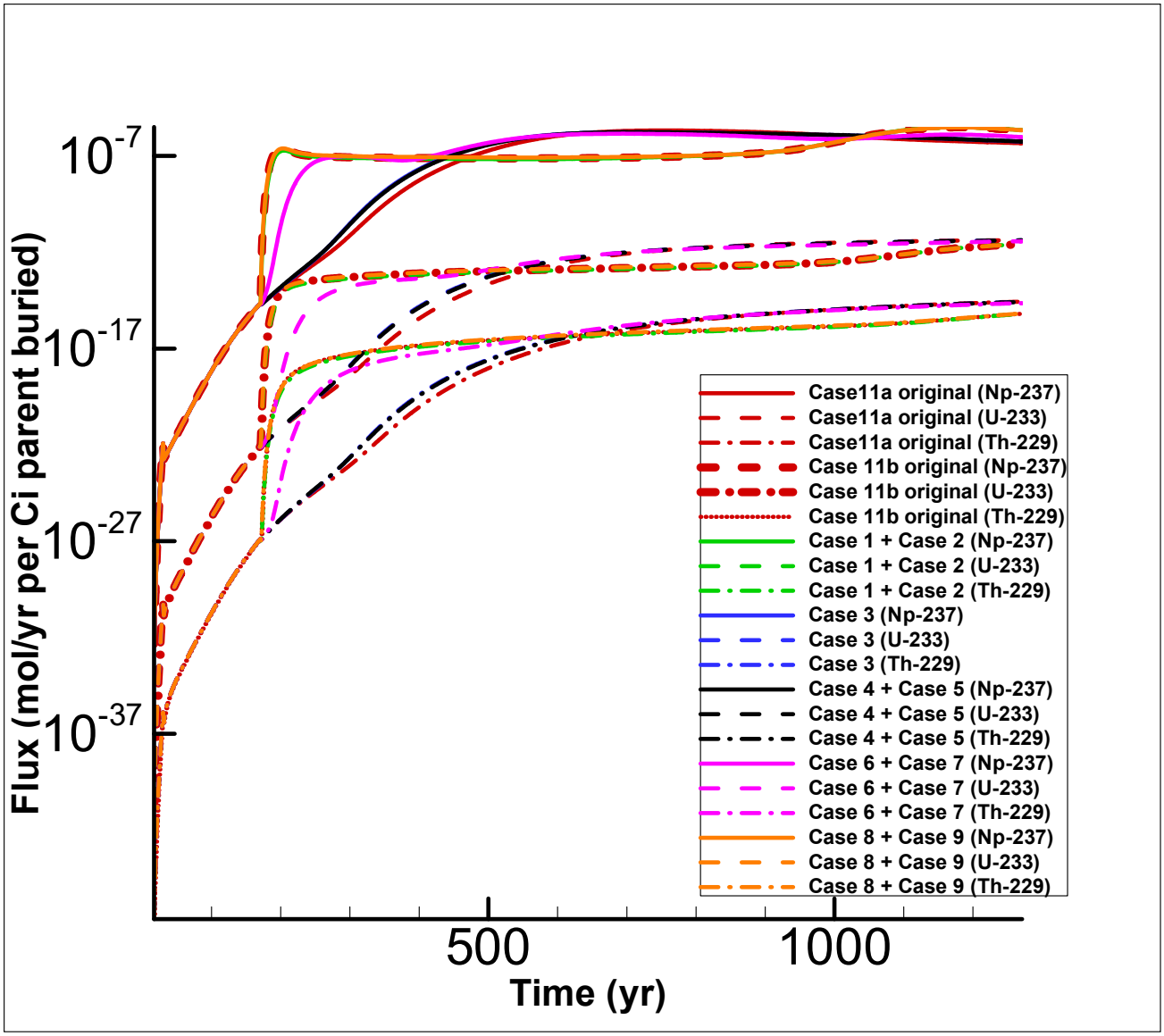

Figure 16. Comparison Am-241 (progeny) flux-to-the-water-table results. (Note: progeny of Am-241 are the same as the Np-237 chain)

Appendix A

In a simulation setup with 2% subsidence applied to only one slope, in the form of an averaged infiltration rate or a discrete hole back-calculated rate, the infiltration rate for the slope-length-weighted, cap-averaged 2% subsidence infiltration rate (Table 1) must be used to calibrate the infiltration rates so that a water mass balance is maintained. Therefore, starting with the slope-length-weighted, cap-averaged infiltration rate formulation:

$$I_{Av-Cap} = \frac{I_{Av-SS} L_{ShortSlope} + I_{Av-LS} L_{LongSlope}}{L_{Total}}$$

For a 2% subsided averaged infiltration rate applied only to the long slope, with the remainder of the cap given an intact infiltration rate:

$$I_{Av-SS} \rightarrow I_{Intact}$$

Substituting and rearranging to solve for I_{Av-LS}:

$$I_{Av-LS} = I_{Av-LS}^{MB} = \frac{I_{Av-Cap} L_{Total} - I_{Intact} L_{ShortSlope}}{L_{LongSlope}}$$

For a 2% subsided averaged infiltration rate applied only to the short slope, with the remainder of the cap given an intact infiltration rate:

$$I_{Av-LS} \rightarrow I_{Intact}$$

Substituting and rearranging to solve for I_{Av-SS}:

$$I_{Av-SS} = I_{Av-SS}^{MB} = \frac{I_{Av-Cap} L_{Total} - I_{Intact} L_{LongSlope}}{L_{ShortSlope}}$$

For a 2% subsided infiltration rate applied to a discrete hole, with the rest of the cap given an intact infiltration rate, we start with the formulation of I_{Av-Cap} :

$$I_{Av-Cap} = \frac{I_{Av-SS} L_{ShortSlope} + I_{Av-LS} L_{LongSlope}}{L_{Total}}$$

and to generally solve for a back-calculated discrete hole infiltration rate:

$$I_{Av-Cap} = \frac{I_{Intact}L_{Intact} + I_{Subsided}L_{Subsided}}{L_{Total}}$$

$$I_{Subsided} = \frac{I_{Av-Cap}L_{Total} - I_{Intact}L_{Intact}}{L_{Subsided}}$$

Substituting:

$$I_{Subsided} = \frac{\frac{I_{Av-SS}L_{ShortSlope} + I_{Av-LS}L_{LongSlope}}{L_{Total}}L_{Total} - I_{Intact}L_{Intact}}{L_{Subsided}}$$

$$I_{Subsided} = \frac{I_{Av-SS}L_{ShortSlope} + I_{Av-LS}L_{LongSlope} - I_{Intact}L_{Intact}}{L_{Subsided}}$$

If the hole is on the long slope:

$$I_{Av-SS} \rightarrow I_{Intact}$$

and therefore:

$$I_{Av-LS} \rightarrow I^{MB}_{Av-LS}$$

Substituting:

$$I_{Subsided} = I^{MB}_{BC-LS} = \frac{I_{Intact}L_{ShortSlope} + I^{MB}_{Av-LS}L_{LongSlope} - I_{Intact}L_{Intact}}{L_{Subsided}}$$

If the hole is on the short slope:

$$I_{Av-LS} \rightarrow I_{Intact}$$

and therefore:

$$I_{Av-SS} \rightarrow I^{MB}_{Av-SS}$$

Substituting:

$$I_{Subsided} = I^{MB}_{BC-SS} = \frac{I^{MB}_{Av-SS}L_{ShortSlope} + I_{Intact}L_{LongSlope} - I_{Intact}L_{Intact}}{L_{Subsided}}$$

References

ACRi (2010) PORFLOW Version 6.3 User's Manual, Revision 3. Analytical & Computational Research, Inc., Los Angeles, CA.

Hamm, L. L., Aleman, S. E., Danielson, T. L., and Butcher, B.T. (2018) Unreviewed Disposal Question Evaluation: Impact of Updated GSA Flow Model on E-Area Low-Level Waste Facility Groundwater Performance. SRNL-STI-2018-00624, Rev. 0. Savannah River National Laboratory, Aiken, SC.

Dyer, J. A. (2018) Conceptual Modeling Framework for E-Area PA HELP Infiltration Model Simulations. SRNL-STI-2017-00678, Rev. 0. Savannah River National Laboratory, Aiken, SC.

Dyer, J. A., and Flach, G. P. (2018) Infiltration Time Profiles for E-Area LLWF Intact and Subsidence Scenarios. SRNL-STI-2018-00327, Rev. 0. Savannah River National Laboratory, Aiken, SC.

Dixon, K. L. (2017) HELP 4.0 Documentation Updates for Software and Data. SRNL-STI-2017-00104, Rev. 0. Savannah River National Laboratory, Aiken, SC.

WSRC (2008) E-Area Low-Level Waste Facility DOE 435.1 Performance Assessment. WSRC-STI-2007-00306, Rev. 0. Washington Savannah River Company LLC, Aiken, SC.

Page Intentionally Left Blank

Distribution List

S. E. Aleman, 735-A
B. T. Butcher, 773-42A
D. A. Crowley, 773-42A
T. L. Danielson, 773-42A
K. L. Dixon, 773-42A
J. A. Dyer, 773-42A
L. L. Hamm, 735-A
N. V. Halverson, 773-42A
T. Hang, 773-42A
C. C. Herman, 773-A
J. J. Mayer, 999-W
R. L. Nichols, 773-42A
A. P. Fellinger, 773-42A
T. S. Whiteside, 773-42A
J. L. Wohlwend, 773-42A
T. N. Foster, EM File, 773-42A – Rm. 243
Records Management (EDWS)